

Characterisation of the n_TOF 20 m beam line at CERN with the new spallation target

J. A. Pavón-Rodríguez^{1,2}, V. Alcayne³, S. Amaducci⁴, M. Bacak², A. Casanovas⁵, M. A. Cortés-Giraldo¹, F. García-Infantes^{6,2}, J. Lerendegui-Marco⁵, A. Manna^{7,8}, E. Musacchio-Gonzalez⁹, N. Patronis¹⁰, M. Sabaté-Gilarte², M. E. Stamati^{10,2}, L. Tassan-Got², V. Vlachoudis², O. Aberle², S. Altieri^{11,12}, H. Amar Es-Sghir⁶, J. Andrzejewski¹³, V. Babiano-Suarez⁵, J. Balibrea⁵, S. Bennett¹⁴, A. P. Bernardes², E. Berthoumieux¹⁵, D. Bosnar¹⁶, M. Busso^{17,18}, M. Caamaño¹⁹, F. Calviño²⁰, M. Calviani², D. Cano-Ott³, D. M. Castelluccio^{21,7}, F. Cerutti², G. Cescutti^{22,23}, S. Chasapoglou²⁴, E. Chiaveri^{2,14}, P. Colombetti^{25,26}, N. Colonna²⁷, P. C. Console Camprini^{21,7}, G. Cortés²⁰, L. Cosentino⁴, S. Cristallo^{17,28}, M. Di Castro², D. Diacono²⁷, M. Diakaki²⁴, M. Dietz²⁹, C. Domingo-Pardo⁵, R. Dressler³⁰, E. Dupont¹⁵, I. Durán¹⁹, Z. Eleme¹⁰, S. Fargier², B. Fernández-Domínguez¹⁹, P. Finocchiaro⁴, S. Fiore^{21,31}, V. Furman³², A. Gawlik-Ramięga¹³, G. Gervino^{25,26}, S. Gilardoni², E. González-Romero³, C. Guerrero¹, F. Gunsing¹⁵, C. Gustavino³¹, J. Heyse³³, D. G. Jenkins³⁴, E. Jericha³⁵, A. Junghans³⁶, Y. Kadi², T. Katabuchi³⁷, I. Knapová³⁸, M. Kokkoris²⁴, Y. Kopatch³², M. Krůčka³⁸, D. Kurtulgil³⁹, I. Ladarescu⁵, C. Lederer-Woods⁴⁰, G. Lerner², T. Martínez³, A. Masi², C. Massimi^{7,8}, P. Mastinu⁹, M. Mastromarco^{27,41}, F. Matteucci^{22,23}, E. A. Mauger³⁰, A. Mazzone^{27,42}, E. Mendoza³, A. Mengoni^{21,7}, V. Michalopoulou^{24,2}, P. M. Milazzo²², R. Mucciola^{17,18}, F. Murtas^{†43}, A. Musumarra^{44,45}, A. Negret⁴⁶, A. Oprea⁴⁶, P. Pérez-Maroto¹, M. G. Pellegriti⁴⁴, J. Perkowski¹³, C. Petrone⁴⁶, L. Piersanti^{17,28}, E. Pirovano²⁹, S. Pomp⁴⁷, I. Porras⁶, J. Praena^{6,2}, N. Protti^{11,12}, J. M. Quesada¹, T. Rauscher⁴⁸, R. Reifarth³⁹, D. Rochman³⁰, Y. Romanets⁴⁹, F. Romano⁴⁴, C. Rubbia², A. Sánchez³, P. Schillebeeckx³³, D. Schumann³⁰, A. Sekhar¹⁴, A. G. Smith¹⁴, N. V. Sosnin⁴⁰, M. Spelta^{7,8}, G. Tagliente²⁷, A. Tarifeño-Saldivia²⁰, D. Tarrío⁴⁷, N. Terranova^{21,43}, P. Torres-Sánchez⁶, S. Urlass^{36,2}, S. Valenta³⁸, V. Variale²⁷, P. Vaz⁴⁹, D. Vescovi³⁹, R. Vlastou²⁴, A. Wallner⁵⁰, P. J. Woods⁴⁰, T. Wright¹⁴, and P. Žugec¹⁶

and the n_TOF Collaboration

¹Universidad de Sevilla, Spain

²European Organization for Nuclear Research (CERN), Switzerland

³Centro de Investigaciones Energéticas Medioambientales y Tecnológicas (CIEMAT), Spain

⁴INFN Laboratori Nazionali del Sud, Catania, Italy

⁵Instituto de Física Corpuscular, CSIC - Universidad de Valencia, Spain

⁶University of Granada, Spain

⁷Istituto Nazionale di Fisica Nucleare, Sezione di Bologna, Italy

⁸Dipartimento di Fisica e Astronomia, Università di Bologna, Italy

⁹INFN Laboratori Nazionali di Legnaro, Italy

¹⁰University of Ioannina, Greece

¹¹Istituto Nazionale di Fisica Nucleare, Sezione di Pavia, Italy

¹²Department of Physics, University of Pavia, Italy

¹³University of Lodz, Poland

¹⁴University of Manchester, United Kingdom

¹⁵CEA Irfu, Université Paris-Saclay, F-91191 Gif-sur-Yvette, France

¹⁶Department of Physics, Faculty of Science, University of Zagreb, Zagreb, Croatia

¹⁷Istituto Nazionale di Fisica Nucleare, Sezione di Perugia, Italy

¹⁸Dipartimento di Fisica e Geologia, Università di Perugia, Italy

¹⁹University of Santiago de Compostela, Spain

²⁰Universitat Politècnica de Catalunya, Spain

²¹Agenzia nazionale per le nuove tecnologie (ENEA), Italy

²²Istituto Nazionale di Fisica Nucleare, Sezione di Trieste, Italy

²³Department of Physics, University of Trieste, Italy

²⁴National Technical University of Athens, Greece

²⁵Istituto Nazionale di Fisica Nucleare, Sezione di Torino, Italy

²⁶Department of Physics, University of Torino, Italy

²⁷Istituto Nazionale di Fisica Nucleare, Sezione di Bari, Italy

²⁸Istituto Nazionale di Astrofisica - Osservatorio Astronomico di Teramo, Italy

²⁹Physikalisch-Technische Bundesanstalt (PTB), Bundesallee 100, 38116 Braunschweig, Germany

³⁰Paul Scherrer Institut (PSI), Villigen, Switzerland

- ³¹Istituto Nazionale di Fisica Nucleare, Sezione di Roma1, Roma, Italy
³²Joint Institute for Nuclear Research (JINR), Dubna, Russia
³³European Commission, Joint Research Centre (JRC), Geel, Belgium
³⁴University of York, United Kingdom
³⁵TU Wien, Atominstytut, Stadionallee 2, 1020 Wien, Austria
³⁶Helmholtz-Zentrum Dresden-Rossendorf, Germany
³⁷Tokyo Institute of Technology, Japan
³⁸Charles University, Prague, Czech Republic
³⁹Goethe University Frankfurt, Germany
⁴⁰School of Physics and Astronomy, University of Edinburgh, United Kingdom
⁴¹Dipartimento Interateneo di Fisica, Università degli Studi di Bari, Italy
⁴²Consiglio Nazionale delle Ricerche, Bari, Italy
⁴³INFN Laboratori Nazionali di Frascati, Italy
⁴⁴Istituto Nazionale di Fisica Nucleare, Sezione di Catania, Italy
⁴⁵Department of Physics and Astronomy, University of Catania, Italy
⁴⁶Horia Hulubei National Institute of Physics and Nuclear Engineering, Romania
⁴⁷Uppsala University, Sweden
⁴⁸Department of Physics, University of Basel, Switzerland
⁴⁹Instituto Superior Técnico, Lisbon, Portugal
⁵⁰Australian National University, Canberra, Australia

Abstract. The n_TOF facility hosts CERN's pulsed neutron source, comprising two beam lines of different flight paths and one activation station. It is based on a proton beam delivered by the PS accelerator impinging on a lead spallation target. During Long Shutdown 2 (LS2) at CERN (2019-2021), a major upgrade of the spallation target was carried out in order to optimize the performances of the neutron beam. Therefore, the characteristics of n_TOF two experimental areas were investigated in detail. In this work, the focus is on the second experimental area (EAR2), located 20 m above the spallation target. Preliminary results of the neutron energy distribution and beam line energy resolution are presented, compared to previous experimental campaigns and Monte Carlo simulations with the FLUKA code. Moreover, preliminary results of the spatial beam profile measurements are shown.

1 Introduction

The n_TOF Collaboration operates the neutron time-of-flight facility at CERN [1], based on a 20 GeV/c pulsed proton beam impinging on a lead target using water to moderate the energy of the neutrons generated in the spallation process. The facility is characterised by a high-instantaneous neutron beam intensity, high energy resolution and a wide neutron energy spectrum, spanning from sub-thermal to GeV.

The facility comprises two neutron beam lines, the first experimental area (EAR1) [2], in operation since 2001, located at 185 m from the spallation target, nearly in the same direction as the incoming proton beam, and the second experimental area (EAR2) [3, 4], located at 20 m above the target, in a perpendicular direction with respect to the proton beam, commissioned in 2014. Thanks to its shorter flight path, EAR2 features a neutron flux around two orders of magnitude bigger in the thermal region and about 30 times higher in the rest of the neutron energy spectrum compared to EAR1 [5], as well as a better signal-to-background ratio, in the case the background is dominated by the natural activity of the sample. This offers a unique opportunity of performing neutron-induced cross section measurements for isotopes with very short half-life [6] or small cross sections, enabling new challenging measurements in very diverse fields. EAR2 beam line is shown in detail in Figure 1.

In the course of the Long Shutdown 2 (LS2) at CERN (2019-2021), the facility went through a major upgrade

consisting in the installation of a new spallation target [7], shown in Figure 2. It has been designed to fully optimise the features of the EAR2 without detriment of EAR1 performance, unlike the previous one specifically designed for EAR1. In particular, this new target presents a flat lead wedge at the top and a dedicated water container to act as moderator for EAR2. These changes impact the characteristics of the neutron beam, i.e. the neutron flux, the energy resolution and the beam profile. The flux plays a key role in the determination of the energy dependence of the neutron-induced cross section. The energy resolu-

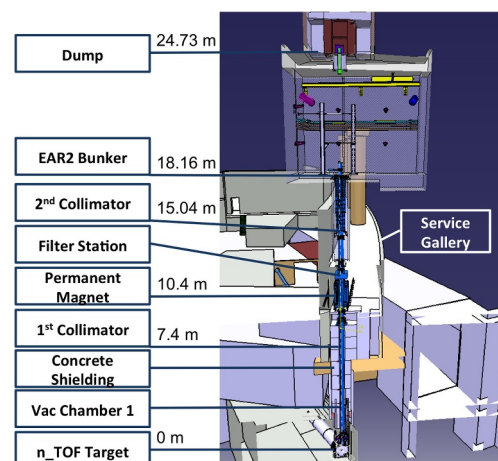


Figure 1: Schematic of EAR2 neutron beam line [4].

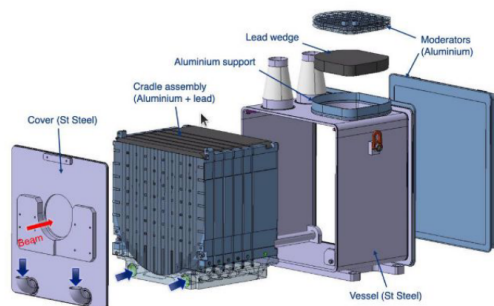


Figure 2: Schematic of the new generation target. The impinging proton beam is indicated with a red arrow. A dedicated lead wedge and moderator's container are observed in the vertical direction [8].

tion is an important constraint in the characterisation of the resonance region of the measured cross sections. And the beam profile determines the size of samples and setups to be used.

During a commissioning phase in 2021, the changes in the characteristics of EAR2 were studied. This work presents the features of the neutron beam with the new spallation target.

2 Neutron flux

The neutron flux measurement was carried out with several detector systems: SiMon (Silicon Monitor) [9], Micromegas (micro-mesh gaseous structure) [10–12], and PPAC (parallel plate avalanche counters) [13, 14]. In Figure 3, a picture of the setup in the experimental hall

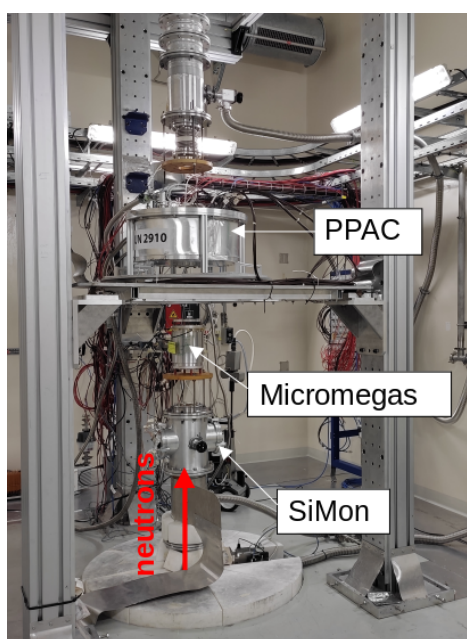


Figure 3: Experimental setup for neutron flux measurement in EAR2.

Table 1: Reaction and energy ranges of interest for each sample.

Detector	Sample	E_{\min} [eV]	E_{\max} [eV]
SiMon	${}^6\text{Li}(n,t){}^4\text{He}$	0.025	1×10^6
PPAC	${}^{238}\text{U}(n,f)$	@ 0.025	1.5×10^5 to 1×10^9
	${}^{235}\text{U}(n,f)$	@ 0.025	1.5×10^5 to 1×10^9
Micromegas	${}^{10}\text{B}(n,\alpha){}^7\text{Li}$	0.025	8×10^3
	${}^{235}\text{U}(n,f)$	@ 0.025	1.5×10^5 to 5.5×10^6
Activation	${}^{197}\text{Au}$	-	4.9

is shown. The neutron beam comes from below, passing through SiMon, then Micromegas, and lastly, PPAC. The detectors are loaded with samples of isotopes whose neutron-induced cross sections for various reactions are considered as standard in different energy regions. The choice of sample and reaction for every detector is summarised in Table 1.

The neutron flux is extracted from the combination of the different data sets in the regions of interest, indicated in Table 1. Moreover, an activation measurement of a ${}^{197}\text{Au}$ sample has been carried out to determine the absolute value of the neutron flux.

In Figure 4 preliminary results of the neutron flux, measured with SiMon and Micromegas, are presented together with Monte Carlo simulations performed with the FLUKA code [15–17]. The results of the previous operational phase, Phase 3 (2014–2018), are also shown for reference. A general increase in the absolute value of the flux can be observed with the new spallation target. More precisely, an increase of 45% is observed at the epithermal region and evaporation peak, while an increase of 25% is observed at the thermal peak.

3 Beam profile

The beam profile is the spatial distribution of the neutrons in the beam. It was measured at 20 m from the target using the position-sensitive PPAC detectors loaded with ${}^{235}\text{U}$. In Figure 5, a preliminary result of this measurement is shown. As can be seen, the beam has a diameter of 5 cm, marked by red dashed lines.

4 Energy resolution

In order to study the energy resolution (ER) in EAR2, C_6D_6 scintillators were used to measure the neutron capture cross section of several isotopes. In Figure 6, a picture of the setup is shown. The cross sections of the various isotopes employed present resonances in a wide energy range and these were used to study the energy resolution at different energy regions. Those regions are indicated in Table 2. In Figure 7a, a first comparison of a resonance in the ${}^{197}\text{Au}(n,\gamma)$ yield measured in the previous operational phase, in 2015, and the current one, in 2021, is shown.

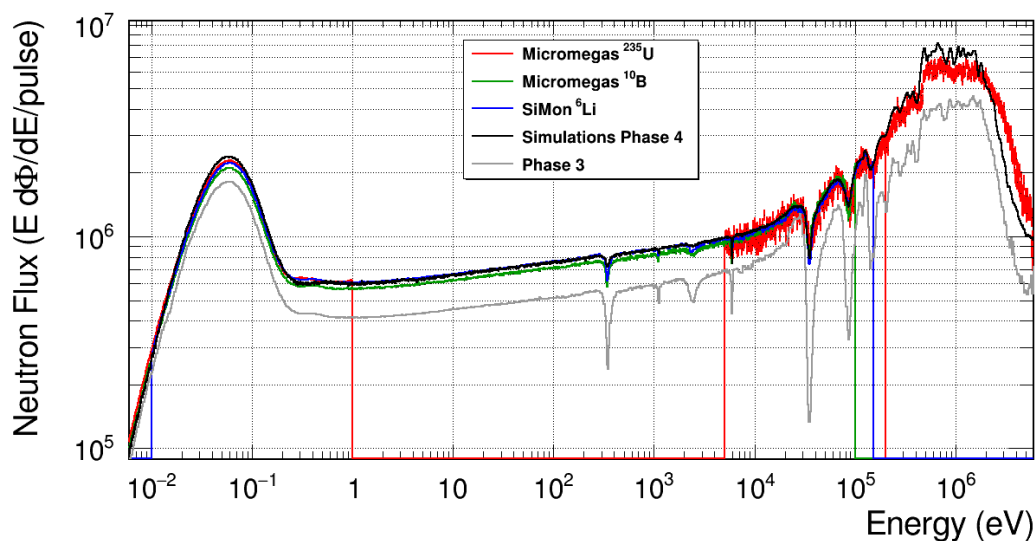


Figure 4: Preliminary experimental neutron flux measured at EAR2 during Phase 4. The flux measurement with Micromegas (red and green histograms) and Silicon (blue) detectors is shown, together with FLUKA simulations. Previous Phase 3 evaluated neutron flux (grey), is also presented for comparison with previous conditions.

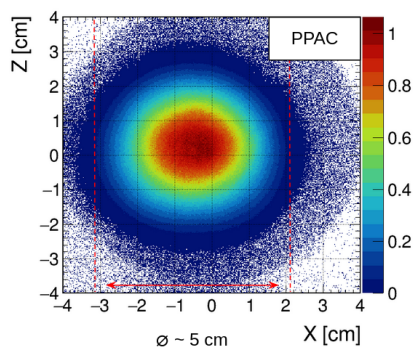


Figure 5: Neutron beam profile measured at EAR2 with PPAC detectors at 20 m from the spallation target.

From this figure, a clear improvement of the resolution is noticeable, as the resonance is narrower. The improved energy resolution in EAR2, together with the recent detector R&D projects [18, 19], opens the way to new and more challenging measurements [20].

The counting rate, as resulting from the measurements, is also compared against the expected yield obtained by means of convoluting the ENDF/B-VIII.0 evaluation [21] with the resolution function. The latter is extracted from FLUKA simulations of the whole neutron production and moderation process in the spallation target. In Figure 7b, a measured resonance of $^{197}\text{Au}(n,\gamma)$ is compared against its expected yield.

5 Summary

During LS2 at CERN, a new spallation target was installed at the n_TOF Facility, requiring a complete study of the

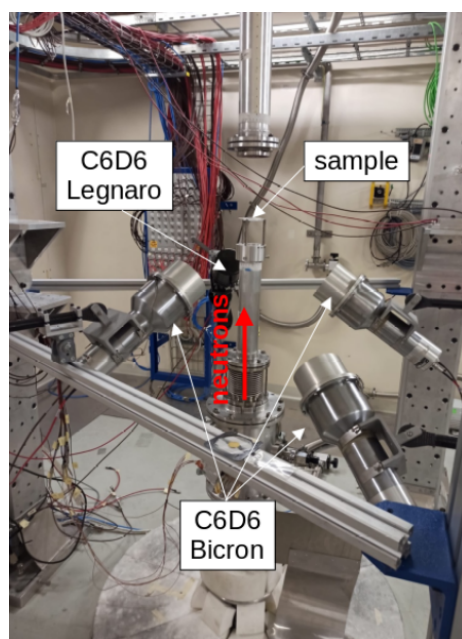


Figure 6: Energy resolution setup.

neutron beam features. In this work we have presented the first preliminary results of measurements and simulations devoted to characterise the features of EAR2 at n_TOF, namely: neutron flux, beam profile and energy resolution.

The neutron flux measurements show a general increase in absolute value with respect to the previous phase of operation, with a beam size of 5 cm of diameter at 20 m from the target. On the other hand, the measurement of resonances in neutron capture reactions in ^{197}Au shows a clear improvement in the energy resolution for the new phase of operation. Furthermore, the agreement

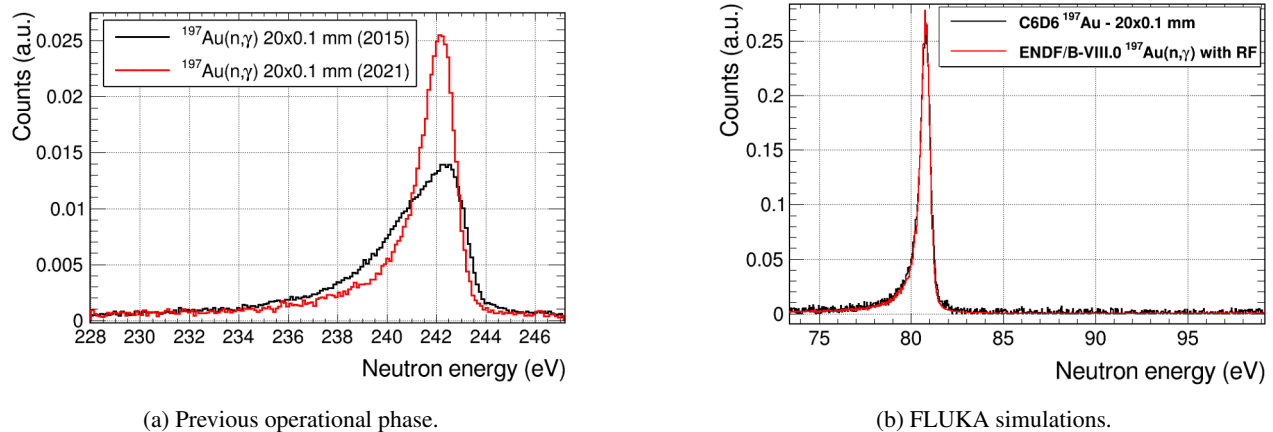


Figure 7: Measurements of resonances in $^{197}\text{Au}(n,\gamma)$ reaction compared with (a) previous operational phase, and (b) the expected $^{197}\text{Au}(n,\gamma)$ yield obtained by means of convoluting the ENDF/B-VIII.0 evaluation with the resolution function as extracted from FLUKA simulations. The shift in energy observed in (b) is due to the effect of the resolution function.

Table 2: Energy ranges of interest for each sample.

Detector	Sample	Goal
	^{197}Au	ER @ 5 eV - 500 eV
C6D6	nat-U	ER @ 6 eV - 500 eV
	nat-Ir	ER < 1 eV
	nat-Fe	ER @ 1 keV - 50 keV
	^{77}Se	ER @ 500 eV - 5 keV

with Monte Carlo FLUKA simulations is highly promising for extracting resonance parameters from EAR2 measurements.

References

- [1] C. Rubbia, S.A. Andriamonje, D. Bouvet-Bensimon, S. Buono, R. Cappi, P. Cennini, C. Gelès, I. Goulas, Y. Kadi, P. Pavlopoulos et al., Tech. rep., CERN, Geneva (1998)
- [2] Guerrero, C., Tsinganis, A., Berthoumieux, E., Barbagallo, M., Belloni, F., Günsing, F., Weiß, C., Chiaveri, E., Calviani, M., Vlachoudis, V. et al., Eur. Phys. J. A **49**, 27 (2013)
- [3] N. Colonna, F. Günsing, E. Chiaveri, Nuclear Physics News **25**, 19 (2015)
- [4] C. Weiß, E. Chiaveri, S. Girod, V. Vlachoudis, O. Aberle, S. Barros, I. Bergström, E. Berthoumieux, M. Calviani, C. Guerrero et al., Nuclear Instruments and Methods in Physics Research Section A: Accelerators, Spectrometers, Detectors and Associated Equipment **799**, 90 (2015)
- [5] Sabaté-Gilarte, M., Barbagallo, M., Colonna, N., Günsing, F., Zucec, P., Vlachoudis, V., Chen, Y. H., Stamatopoulos, A., Lerenegui-Marco, J., Cortés-Giraldo, M. A. et al., Eur. Phys. J. A **53**, 210 (2017)
- [6] M. Barbagallo, A. Musumarra, L. Cosentino, E. Maugeri, S. Heinitz, A. Mengoni, R. Dressler, D. Schumann, F. Käppeler, N. Colonna et al. (n_TOF Collaboration), Phys. Rev. Lett. **117**, 152701 (2016)
- [7] R. Esposito, M. Calviani, O. Aberle, M. Barbagallo, D. Cano-Ott, T. Coiffet, N. Colonna, C. Domingo-Pardo, F. Dragoni, R. Franqueira Ximenes et al. (for the n_TOF Collaboration), Phys. Rev. Accel. Beams **24**, 093001 (2021)
- [8] M. Bacak, *Design, construction, commissioning and early operation of the third-generation n_TOF neutron spallation target at CERN* (15th International Conference on Nuclear Data for Science and Technology, 2022)
- [9] L. Cosentino, A. Musumarra, M. Barbagallo, N. Colonna, L. Damone, A. Pappalardo, M. Piscopo, P. Finocchiaro, Review of Scientific Instruments **86**, 073509 (2015), <https://doi.org/10.1063/1.4927073>
- [10] Y. Giomataris, P. Rebourgeard, J. Robert, G. Charpak, Nuclear Instruments and Methods in Physics Research Section A: Accelerators, Spectrometers, Detectors and Associated Equipment **376**, 29 (1996)
- [11] S. Andriamonje, M. Calviani, Y. Kadi, R. Losito, V. Vlachoudis, E. Berthoumieux, F. Günsing, A. Giganon, Y. Giomataris, C. Guerrero et al., J. Korean Phys. Soc. **59**, 1597 (2011)
- [12] I. Giomataris, R.D. Oliveira, Patent CEA-CERN, Application Number 09 290 825.0 (2009)
- [13] C. Paradela, L. Tassan-Got, L. Audouin, B. Berthier, I. Duran, L. Ferrant, S. Isaev, C. Le Naour, C. Stephan, D. Tarrío et al. (n_TOF Collaboration), Phys. Rev. C **82**, 034601 (2010)
- [14] D. Tarrío, L. Tassan-Got, L. Audouin, B. Berthier, I. Duran, L. Ferrant, S. Isaev, C. Le Naour, C. Pa-

- radela, C. Stephan et al. (n_TOF Collaboration), Phys. Rev. C **83**, 044620 (2011)
- [15] <https://fluka.cern>
- [16] C. Ahdida, D. Bozzato, D. Calzolari, F. Cerutti, N. Charitonidis, A. Cimmino, A. Coronetti, G.L. D'Alessandro, A.D. Servelle, L.S. Esposito et al., Frontiers in Physics **9** (2022)
- [17] G. Battistoni, T. Boehlen, F. Cerutti, P.W. Chin, L.S. Esposito, A. Fassò, A. Ferrari, A. Lechner, A. Empl, A. Mairani et al., Annals of Nuclear Energy **82**, 10 (2015)
- [18] V. Alcayne, *A segmented total energy detector (sTED) for (n, γ) cross section measurements at n_TOF EAR2* (15th International Conference on Nuclear Data for Science and Technology, 2022)
- [19] C. Domingo-Pardo, V. Babiano-Suarez, J. Balibrea-Correa, L. Caballero, I. Ladarescu, J. Lerendegui-Marco, J.L. Tain, A. Tarifeño-Saldivia, O. Aberle, V. Alcayne et al., arXiv: 2208.02163 (2022)
- [20] J. Lerendegui-Marco, *New perspectives for neutron capture measurements in the upgraded CERN-n_TOF Facility* (15th International Conference on Nuclear Data for Science and Technology, 2022)
- [21] D. Brown, M. Chadwick, R. Capote, A. Kahler, A. Trkov, M. Herman, A. Sonzogni, Y. Danon, A. Carlson, M. Dunn et al., Nuclear Data Sheets **148**, 1 (2018)